Journal of Hazardous Materials 355 (2018) 104–110

Contents lists available at ScienceDirect

Journal of Hazardous Materials

journal homepage: www.elsevier.com/locate/jhazmat

Impacts of initial temperature and cylindrical obstacles on the dispersing flammable limits of accidental methane releases in an LNG bunkering terminal

Byung Chul Choi[a,*], Kweon-Ha Park[b], Deog-Hee Doh[b]

[a] R&D Center, Korean Register of Shipping, Busan 46762, Republic of Korea
[b] Division of Mechanical Engineering, Korea Maritime & Ocean University, Busan 49112, Republic of Korea

ARTICLE INFO

Keywords:
LNG dispersion
Flammable limits
Vorticity
Cold gas temperature
Cylindrical obstacle

ABSTRACT

This paper presents a numerical study on the dispersing flammable limits with respect to the initial methane releases at $T_{CH4,0}$ = −50 and −150 °C in the crosswind of ambient air according to the arrangement of (a) No Tank, (b) Tank I, (c) Tank II, and (d) Tank I and II on the ground. To provide a better physical insight on the dispersion behaviors of the methane releases, the spatial distributions of the quasi-averaged methane concentration and flow fields were mainly analyzed using 3-D large eddy simulations. Consequently, the results of both the parameters can be summarized in that the vortex characteristics of the rotating direction and vorticity generated by the interactions not only between the crosswind and cylindrical obstacles but also between the crosswind and releasing methane flows played important roles in determining the dispersing flammable limits depending on the mixing characteristics.

1. Introduction

Liquefied natural gas (LNG) as an alternative marine fuel offers environmental benefits that can satisfy the strict regulations for controlling environmental pollutants from internal combustion engines of ocean-going vessels. To supply LNG fuel to the increasing number of LNG-fueled vessels, a safe and cost-effective infrastructure of LNG bunkering should be globally constructed. A safe design to mitigate potential fire and explosion hazards caused by the flammable LNG releases is one of the essential issues. In this respect, the International Code of Safety for Ships using Gases or Low-flashpoint Fuels (IGF Code) has been mandatory since 2017 to minimize the risk to the crew, environment, or ship structure [1]. A consequence modeling and analysis using computational fluid dynamics (CFD) will be the most suitable technique in determining the flammable extent of LNG releases [2,3], to specify the safety actions, e.g., gas detection, safety and security zones as well as prevention and protection systems.

The arrangement of land-based facilities for LNG storage and transfer systems should also be based on an exclusion zone to protect the public from flammable gas dispersions. Specifically, a dispersion exclusion zone is required by the U.S. regulation of 49 CFR 193 [4], which incorporates the National Fire Protection Association (NFPA) 59 A to determine accidental spills [5]. However, various technical approaches are constantly being studied particularly for predicting flammable gas dispersions realistically. Several parameters influencing vapor dispersions of LNG released on water and dry concrete were widely investigated using CFD simulations, mainly considering the LNG source interacting with turbulence effect due to wind entrainment [6]. The appearance of turbulent kinetic energy generated with a wind profile by a vapor fence within vapor barriers was described with methane gas concentrations, compared with the case without any impoundment [7]. In the presence of obstacles, the application of a turbulence model is the key to a successful simulation of the dense gas dispersion [8]. Advanced implementations in numerical models have been updated to enhance the prediction accuracy of the dispersion behaviors, such as two-phase LNG releases [9], phase change of water vapor in air [10], and buoyancy effect on turbulence [11]. On the other hand, a simple methodology to perform a consequence analysis for diverse scenarios of LNG releases has been proposed for deep-water port facilities after reviewing the various models of spills and dispersions [12].

To enhance understanding of the flammable extent of LNG releases, the objective of this study is to characterize the dispersion behaviors of a comprehensive combination of LNG releases considering the variations in initial methane temperature and the presence of cylindrical obstacles, and to identify the importance of the vortical structure

* Corresponding author.
E-mail address: byungchul.choi@hotmail.com (B.C. Choi).

https://doi.org/10.1016/j.jhazmat.2018.05.021
Received 25 October 2017; Received in revised form 9 May 2018; Accepted 10 May 2018

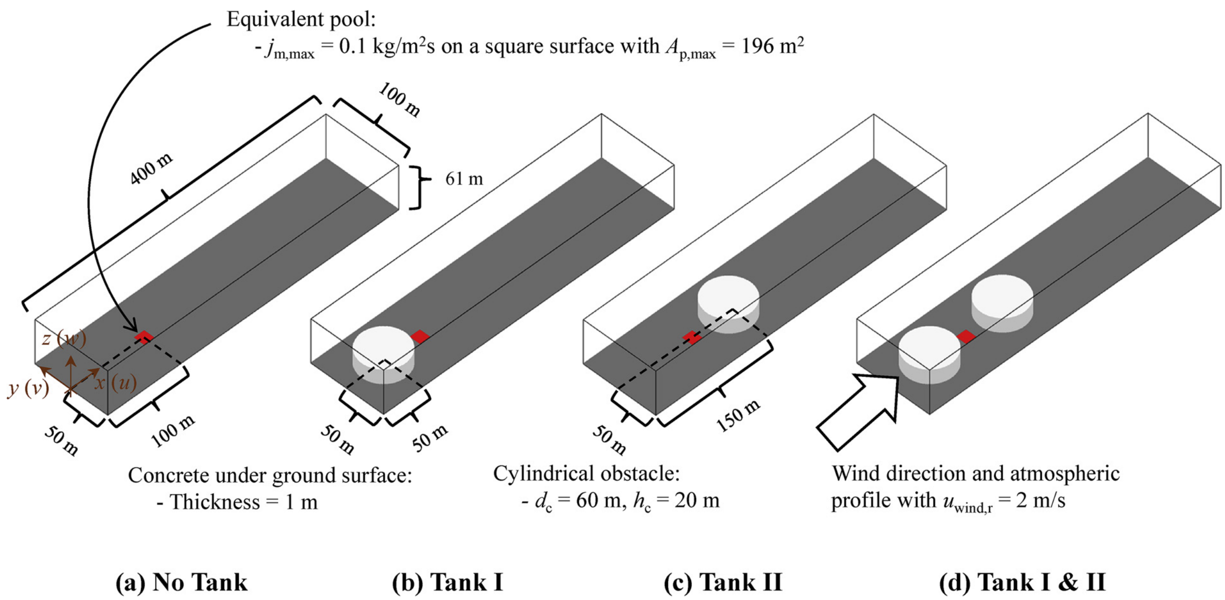

Fig. 1. Schematic of calculation domains for Tank I and II.

resulting from the change in two parameters for determining the extent of the lean flammable limits (LFLs) regulated by the IGF code [1].

2. Numerical methods

To conduct simulations for typical LNG receiving and bunkering terminals located on land, the calculation domains were simply modeled with cylindrical obstacles on a plane using PyroSim [13]. As shown in Fig. 1, A three-dimensional $400 \times 100 \times 61$ (m^3) domain was set with a square liquid pool centered at (100, 50, 1) and marked with red color. Tank I and Tank II as cylindrical obstacles marked with white-gray color are consistent with the general shape of an LNG containment on land with a diameter of $d_c = 60$ m and height of $h_c = 20$ m. These tanks were artificially centered at (50, 50, 1) and (150, 50, 1), considering a representative combination of the relative leak locations with respect to the tanks against a forced wind boundary. The ground was modeled as a solid body with a concrete material surface at the bottom *x-y* plane of 1 m thickness, marked with dark gray color. The calculation domain was discretized by Cartesian grid cells with a finite volume of $0.5 \times 0.5 \times 0.5$ (m^3), which was selected after the verification of grid dependencies with four cubic grids of 2.0, 1.0, 0.5, and 0.2 (m) finer than the used in the model validation [15–18]. The total number of cells of 19,520,000 was used for the uniform mesh, in which the ratio of cell size was unified as 1 for the *x*, *y*, and *z* cells.

The liquid pool was modeled that the gas-phase methane fuel was perpendicularly released with $j_{m,max} = 0.1$ kg/m²·s on a square shape with an equivalent area of 196 m² (see supplementary material A for details). Using the Fire Dynamics Simulator (FDS) as a large eddy simulation (LES) code [14], which was successfully validated with the LNG dispersion and spill tests [15–18], dispersion simulations were conducted with respect to the representative temperatures of $T_{CH4,0} = -50$ and -150 °C to compare the gravitational effect. The initial wind profile was generated by a power law with the reference wind velocity of 2.0 m/s [4]. The initial temperature of the ambient air was set as $T_{g,0} = 26.85$ °C with a relative humidity of 50% [4]. The results were temporarily averaged for 30 s before the 600 s calculation, as a quasi-averaged state (see supplementary material B for details).

3. Results and discussion

The overall spatial distributions of the quasi-averaged methane concentration considerably matched with those of the quasi-averaged gas temperature (see supplementary material C for details). Dispersion behaviors in the *x-y* plane were analyzed for $z = 10$ and 30 m at the $T_{CH4,0} = -50$ °C and for $z = 1$ and 10 m at the $T_{CH4,0} = -150$ °C, according to the arrangement of Tank I and II (see supplementary material D for details). In the following, the quasi-averaged methane concentration fields are mainly discussed with the quasi-averaged flow fields in the *x-z* plane.

3.1. Dispersion behaviors of the $T_{CH4,0} = -50$ °C

Fig. 2 shows the spatial distributions of quasi-averaged methane concentration for $T_{CH4,0} = -50$ °C in the *x-z* plane at $y = 0$, according to the arrangement of the cylindrical obstacles. For Fig. 2(a) No tank, following the center trajectory defined as a streamline which starts from a point of $z = 1$ m above the pool center, the quasi-averaged methane concentration gradually decreased because of the dilution of methane release with crosswind. Particularly, the spatial distribution of quasi-averaged methane concentration was relatively wider in the upwind side (left hand) of the center trajectory than in the downwind side (right hand). The spatial profile of the contour of 20% LFL reached up to $\Delta x \approx 72$ m at a height of $z \approx 38$ m, in which Δx was defined as the extent of horizontal distance from the pool center of $x = 100$ m to the contour of 20% LFL.

For Fig. 2(b) Tank I, the center trajectory moved toward the downwind direction staying very close to the ground after the methane gas was released. On the other hand, the spatial profile of contour of 20% LFL moved toward the upwind direction, staying near to the rearward wall of the cylindrical obstacle. The contour of 20% LFL showed a wider dispersion than that in Fig. 2(a) because of the cylindrical obstacle, and it reached up to $\Delta x \approx 112$ m in the downwind direction. For Fig. 2(c) Tank II, the center trajectory trailed across the top of the cylindrical obstacle and then rotated in the clockwise direction behind the obstacle. The spatial profile of the contour of 20% LFL that was distributed along the center trajectory reached up to $\Delta x \approx 185$ m behind the cylindrical obstacle at a height of $z \approx 45$ m. For Fig. 2(d) Tank I & II, the center trajectory formed a vortex between Tank I and Tank II in the clockwise direction and rotated toward the center of the vortex. Consequently, the spatial profile of the contour of 20% LFL became detached from the square pool while the contours of 20–60% LFL stayed very close to the upper part of the rearward wall of Tank I.

Fig. 3 shows the quasi-averaged flow fields in response to the